

## Original Article

# Cranial variation between coastal and offshore bottlenose dolphins, *Tursiops truncatus* (Cetacea: Delphinidae) in Ecuador and the Mediterranean: a three-dimensional geometric morphometric study

Morgane Dromby<sup>1</sup>, Fernando Félix<sup>2,3</sup>, Ben Haase<sup>3</sup>, Paulo C. Simões-Lopes<sup>4</sup>, Ana P.B. Costa<sup>4,5</sup>, Aude Lalis<sup>6</sup>, Celine Bens<sup>7</sup>, Michela Podestà<sup>8</sup>, Giuliano Doria<sup>9</sup>, Andre E. Moura<sup>1,\*</sup>

<sup>1</sup>Museum and Institute of Zoology PAS, ul. Wilcza 64, 00-679 Warszawa, Poland

<sup>2</sup>Pontificia Universidad Católica del Ecuador (PUCE), Ave 12 de Octubre 1076, 170143 Quito, Ecuador

<sup>3</sup>Museo de Ballenas, Av. General Enriquez Gallo, entre calles 47 y 50, Salinas, Ecuador

<sup>4</sup>Federal University of Santa Catarina, R. Eng. Agrônomo Andrei Cristian Ferreira, s/n - Trindade, 88040-900, Florianópolis, SC, Brazil

<sup>5</sup>Rosenstiel School of Marine, Atmospheric, and Earth Science, University of Miami, 1365 Memorial Drive, 33146, Coral Gables, Florida, USA

<sup>6</sup>Institut de Systématique, Évolution, Biodiversité (ISYEB), Muséum national d'Histoire naturelle, CNRS, Sorbonne Université, EPHE, Université des Antilles, CP51, 57 rue Cuvier, 75005 Paris, France

<sup>7</sup>Muséum National d'Histoire Naturelle, UMR CNRS 5202, 55 rue Buffon, 75000 Paris, France

<sup>8</sup>Museum of Natural History of Milan, corso Venezia 55, 20121 Milan, Italy

<sup>9</sup>Museo Civico di Storia Naturale 'Giacomo Doria', Via Brigata Liguria 9, I-16121 Genova, Italy

\*Corresponding author. Ornithological Station (MIZ-PAS), ul. Nadwiślańska 108, 80-680 Gdańsk, Poland. E-mail: [amoura@miiz.waw.pl](mailto:amoura@miiz.waw.pl)

## ABSTRACT

Skull shape analysis provides useful information on wildlife ecology and potential local adaptations. Common bottlenose dolphins (*Tursiops truncatus*) often differentiate between coastal and offshore populations worldwide, and skull shape analyses can be particularly useful in this context. Here we quantify skull shape variation between coastal populations from the Gulf of Guayaquil (Ecuador) and the Mediterranean Sea, compared to offshore specimens from multiple oceans. We analysed skull shape differences using 3D models from museum specimens through geometric morphometrics (3DGM). Two complementary landmark approaches included single-point semi-landmarks in homologous features, as well as pseudo-landmarks placed automatically. Results show skull shape distinction between both coastal populations and offshore specimens. Offshore specimens showed little differentiation between distinct locations. Skull shape patterns mostly diverged in the shape and length of rostrum, as well as the shape of the ascending processes of the maxilla, pterygoids, and occipital bones. However, both coastal populations differed in the patterns and direction of change of those features and were also morphologically distinct. Our results are consistent with local data on site fidelity and social structure in the coastal populations. Skull shape changes suggest divergent feeding and sound production patterns are potential drivers, probably specific to the local environment of each community.

**Keywords:** 3DGM; ecotypes; morphology; photogrammetry; skull shape

## INTRODUCTION

Mammals are ecologically diverse animals, and their highly variable skull shape can provide a wealth of information regarding the ecology, evolutionary history, and taxonomy of the animals (e.g. Smith 2006; Costa *et al.* 2016; Machado 2020). Therefore, analyses of skull variation and its geographical

structure can provide an important contribution to our understanding of the evolutionary ecology and biogeography of wild animals, particularly in taxa where other data are challenging to acquire.

The bottlenose dolphin (*Tursiops truncatus* Montagu, 1821) is a cosmopolitan, polymorphic, and widely recognized dolphin

species. Throughout its range, researchers have described a distinction between coastal and offshore ecotypes based on multiple criteria. Cranial features, in particular, can be used to distinguish many coastal bottlenose dolphin populations from offshore dolphins. For example, along the west coast of the United States, coastal specimens have narrower internal nares and palatine width, and a higher number of teeth (Perrin *et al.* 2011). Along the east coast of the United States, coastal dolphins can also be distinguished from offshore dolphins based on relative length of internal nares, condylobasal length, and zygomatic width (Kenney 1990; Mead and Potter 1995), while having a smaller skull on average (Mead and Potter 1995; Costa *et al.* 2022). They also have distinct physiological signatures and parasitological patterns when compared to their offshore counterparts (Hersh and Duffield 1990; Mead and Potter 1995; Costa *et al.* 2022). Differences in skull structures have also been found in specimens from the south-eastern Pacific with coastal specimens having shorter anteorbital processes, narrow palatine bones, wide and fragile pterygoids with a rounded apex, and broad separation between the occipital condyles (Van Waerebeek *et al.* 1990).

Coastal dolphins are often found in distinct shallow areas and often show high site fidelity to bays and estuaries, while offshore dolphins are thought to be part of a single unstructured population found in pelagic, nearshore and insular waters worldwide (e.g. Hoelzel *et al.* 1998; Natoli *et al.* 2004; Sellas *et al.* 2005; Parsons *et al.* 2006; Quérrouil *et al.* 2007; Tezanos-Pinto *et al.* 2009; Costa *et al.* 2016, 2021, 2022; Simões-Lopes *et al.* 2019; Moura *et al.* 2020). This ecological distinction has been suggested to result from distinct foraging habits between coastal and offshore dolphins, as demonstrated by differences in tooth numbers/size (Perrin *et al.* 2011; Costa *et al.* 2016), stable isotopes (Fernández *et al.* 2011; Gibbs *et al.* 2011; Giménez *et al.* 2017; Díaz-Gamboa *et al.* 2018; Pereira *et al.* 2020; Borrell *et al.* 2021), and stomach contents (Barros and Wells 1998; Gannon and Waples 2004; McCabe *et al.* 2010; Gibbs *et al.* 2011; Giménez *et al.* 2017).

Studies on genetics, behaviour and social structure in the south-east Pacific have also identified coastal and offshore populations of bottlenose dolphins in the Gulf of Guayaquil, Ecuador (Félix *et al.* 2017, 2018; Bayas-Rea *et al.* 2018; Félix and Burneo 2020). The coastal population is hierarchically structured, with females grouping with each other and males forming alliances for reproductive purposes (Félix 1997). This population was also seen using specific foraging strategies such as fish stranding (Jimenez and Alava, 2015), in some areas. Studies on mtDNA variation showed that this coastal population is genetically distinct from other coastal and offshore populations living in the south-east Pacific (Bayas-Rea *et al.* 2018). Morphometric studies supported these findings when discerning skull shape between these same populations (e.g. Peru and Ecuador; Santillán *et al.* 2008). However, a comparison with bottlenose dolphins from locations outside the Pacific has not been carried out.

Genetic studies have suggested a similar division in the Mediterranean, with several communities showing high site fidelity to coastal areas with varying degrees of social segregation from dolphins elsewhere. Overall, Mediterranean bottlenose dolphins occupy most coastal waters of the basin and, to a lesser extent, offshore waters around islands and archipelagos (Bearzi *et al.* 2005, 2008). They can form groups of between 4 to

20 individuals, depending on the ecological conditions of specific regions (Forcada *et al.* 2004). Some social groupings were shown to be mostly unstable, regularly changing in composition and size (Bearzi *et al.* 2005), without apparent sexual segregation reported so far (Bearzi *et al.* 1997). However, stable social units have been described in some locations. Most notably, dolphins inhabiting the Ligurian sea have been shown to form two large and stable social units along the coasts of Italy and Corsica that do not often interact with dolphins from elsewhere (Gnone *et al.* 2011; Carnabuci *et al.* 2016). Although no fine-scale data exist for the Ligurian sea, genetic studies elsewhere also found evidence of genetic structure between geographically close regions (Natoli *et al.* 2005; Gaspari *et al.* 2015a, b; Brotons *et al.* 2019). Therefore, multiple studies have referred to the Mediterranean *Tursiops* as having a meta-population structure (Nichols *et al.* 2007; Gaspari *et al.* 2015b; Carnabuci *et al.* 2016), which could include animals with a more typical offshore ecology (Gaspari *et al.* 2015b). However, no information to date exists on potential morphological differentiation between coastal and offshore specimens in the Mediterranean.

In the study of morphological variation, geometric morphometrics (GM) has been shown to be a useful tool to detect potential adaptive skull shape patterns in several vertebrate species and infer their driving factors (Christiansen 2008; Adams 2011; Cooke 2011; Fabre *et al.* 2014; Forrest *et al.* 2018; Borgard *et al.* 2020). One main benefit is that it assesses shape changes in biological forms regardless of size, which can be highly plastic. The method is based on placing key landmarks (LMs) distributed over the structure of interest (Richtsmeier *et al.* 2002). Although traditionally based on two-dimensional (2D) images, increasingly the analyses of three-dimensional shapes are favoured when using GM. Three-dimensional geometric morphometrics (3DGM) limits errors related to distortion effects generated from photographing or translating a 3D object into a 2D image (Buser *et al.* 2018), allowing a more robust evolutionary interpretation of the morphological changes.

Geometric morphometrics has been used previously in the analyses of cetaceans, providing important insights into the patterns and processes determining skull shape changes in several species. This includes understanding of ontogenic patterns in porpoises (Galatius *et al.* 2011), identifying ecological drivers of skull shape evolution across cetaceans (Galatius and Goodall 2016; McCurry *et al.* 2017a, b; Galatius *et al.* 2020), and describing the geographical variation of skull shape within dolphin species (Loy *et al.* 2011; Ngqulana *et al.* 2019b; Nicolosi and Loy 2019). Geometric morphometrics has been used to analyse morphological differentiation in *Tursiops* (e.g. Indian Ocean: Jedensjö *et al.* 2017, 2020; Gray *et al.* 2022; Ngqulana *et al.* 2019a; Brazil: Hohl *et al.* 2020; Mexico: Esteves-Ponte *et al.* 2022), although 3DGM has not yet been used extensively to distinguish skull shape between coastal and offshore ecotypes of bottlenose dolphins. A recent study used 3DGM in combination with other morphological and genetic data to investigate the evolutionary distinction between the ecotypes of the north-west Atlantic, with results supporting distinct species (Costa *et al.* 2022). This shows the potential of 3DGM to identify morphological variation in cetacean skulls. In the south-east Pacific, only 2D morphometric studies exist (Santillán *et al.* 2008), and none was carried out in the Mediterranean region.



**Figure 1.** Map showing sample number of common bottlenose dolphin individuals per location. Offshore populations in dark red, coastal populations from Guayaquil (Ecuador) in purple, coastal populations from the Mediterranean Sea in orange.

In this study, we present the results of our 3DGM analysis on skulls of bottlenose dolphins to identify cranial variation that is congruent with differential habitat use, with a focus on the coastal populations from the Gulf of Guayaquil and the Mediterranean Sea relative to offshore specimens. We test the following hypotheses: is there a significant distinction in skull shape between dolphins showing an offshore vs. coastal ecology in these regions? If so, do the different coastal ecotypes differ in their skull shape depending on location, or do they converge to similar skull shapes due to ecological similarity? We also test if the observed 3D shape changes can be used to predict the potential ecological drivers. Previous studies suggest that feeding habits, communication systems, diving patterns and other environmental factors could be responsible for skull shape patterns in *Tursiops* (e.g. Mead and Potter 1995; Perrin *et al.* 2011; Costa *et al.* 2016), and skull shape changes observed in coastal populations will be interpreted in light of their relevant ecological characteristics.

## MATERIAL AND METHODS

### Data collection

We analysed physically mature skulls of common bottlenose dolphins (*Tursiops truncatus*) kept at the Museo de Ballenas in Salinas (Ecuador), the Museum d'Histoire Naturelle in Paris (France), the Federal University of Santa Catarina (Brazil), the Museum of Natural History of Milan (Italy), and the Museo Civico di Storia Naturale 'Giacomo Doria' in Genova (Italy).

Physically immature specimens were not analysed, since skull shape changes considerably during early life stages in Delphinidae (Perrin and Heyning 1993).

The specimens originated from the south-east Pacific, the Mediterranean Sea, north-east and south-west Atlantic (Fig. 1), and included both putative coastal and confirmed offshore specimens. Putative coastal specimens included those originating from the inner estuary of the Guayaquil Gulf (Ecuador) and the Ligurian and Adriatic seas in the Mediterranean. Offshore specimens were from the coast of Brazil [confirmed as offshore by Costa *et al.* (2016)], and the French Atlantic coast (which, based on previous genetic analyses, are most likely to be of the offshore ecotype; Quérroul *et al.* 2007), and from the central coast of Ecuador north of the Gulf of Guayaquil [as defined by Bayas-Rea *et al.* (2018), based on genetic analysis]. Full details and accession numbers of the specimens used here can be found in the Supporting Information, Table S1. Details regarding habitat classification also available in the Supporting Information, Table S2.

### Image acquisition and three-dimensional modelling

Three-dimensional (3D) models were created for all specimens, using photogrammetric techniques based on 250 to 500 high-resolution digital photographs covering the entire surface of the skull. A standard photographing set-up protocol was replicated for each session to avoid systematic errors related to the equipment and image distortion. Photographs were taken using

a high-resolution DSLR camera (> 8 Megapixel) and ensuring a minimum lateral overlap of 60% and frontal overlap of 80% between consecutive photographs. For each specimen, a fixed focal length was used and kept constant throughout the photography session. Camera shooting settings depended on the lighting conditions in the room and aimed to optimize image sharpness and depth of field by finding a balance between the smallest aperture combined with the highest shutter speed possible.

Three-dimensional reconstruction from digital photographs was done using the open-source photogrammetry software MESHROOM v.2019.2.0 (Griwodz *et al.* 2021). MESHROOM applies a variety of algorithms to identify notable features within each image, which can then be reliably matched between images. Feature matching is then used to identify the relative position of individual photographs in 3D space together with camera specific information, such as focal length. Before model reconstruction, images were edited to improve tonal contrast and sharpening, to isolate the skulls from the background, and to increase the number of notable features visible on the skulls. Features were identified using the SIFT method (Scale-Invariant Feature Transformation; Otero and Delbracio 2014). Because we aimed at producing a 3D model of the entire skull that could be fully rotated, the SIFT\_float method was used. For the feature-matching step, we used the option 'Guided matching', which improves the number of recognized cameras by producing a second stage in the matching procedure. Because the camera positioning changed between photographs, we also disabled the 'Use rig constraint' option. For specimens with < 300 images, we also added the 'Akaze' algorithm for feature identification (Alcantarilla *et al.* 2013) and changed the prescriber preset to 'High' to increase the number of features extracted from the pictures. We also decreased the 'Max Descriptors' and 'Number of matches' to 0, as this maximizes the number of descriptors used for the reconstruction and kept all matches recovered for downstream processing. The Downscale level was set to 1 in the 'Depth Map' node to increase the precision of the modelling, and lowered the 'minimum consistency camera' and the 'minimum consistency camera similarity' to 2 and 3, respectively, to maximize the completeness of the meshes in the final models. Full details of the parameters used during 3D reconstruction can be found in the Supporting Information, Table S3.

### Landmark placement for geometric morphometrics

We performed GM skull shape analyses on the 3D models of 58 adult skull specimens, using two different landmarking strategies: manual and automatic. Manual landmarking is based on the prior selection of multiple landmarks in homologous features that can be placed consistently in all individuals analysed (Richtsmeier *et al.* 2002). It has been used extensively in GM studies to identify variation in specific morphological structures and relate them to other mechanisms, such as ontogenic development, ecologic, taxonomic, or biomechanic differences (Mitteroecker and Gunz 2009; Lawing and Polly 2010; Cooke and Terhune 2015). However, the process requires high precision and is time-consuming. Furthermore, it is typically based on relatively sparse landmark configurations, which can lose important geometric information by missing morphological

features of interest when comparing variation between predefined groups.

Alternatively, automatic landmarking can be used to compensate for the limitations of manual landmarking. It requires less processing time and minimizes errors related to observer subjectivity or natural variability occurring among individuals (Gao *et al.* 2019). Automatic landmarking generates pseudo-landmarks based on point cloud registration, distributed all over the target 3D surface without considering homology. Compared to manual landmarking, it increases the overall surface coverage, which enables the capturing of more biological information. This is especially useful in structures with poor geometric shapes, where homologous points are difficult to determine (Gao *et al.* 2019). However, such methods are 'blind' to biological information and, therefore, carry the risk of more noisy inference when comparing the ecological significance of differences in biological structures. Therefore, in this study the two approaches are used to complement each other.

### Manual landmarking

We imported 3D models into the software IDAV Landmark v.3.0 (Wiley 2005), and digitized 71 single-point LMs in homologous skull features and 340 semi-landmarks based on eight line and three patch guides (Fig. 2; Supporting Information, Table S4). For skulls where some of the target structures were missing (due to post-mortem damage), we used the R-package 'geomorph' (v.3.2.0) to estimate 3D LMs by applying the function 'estimate.missing' with the option thin-plate spline. The technique estimates landmark locations using a thin-plate spline on specimens with missing landmarks by first aligning it with a complete reference individual based on their common set of landmarks (Mitteroecker and Gunz 2009).

### Automatic landmarking

We carried out automatic landmarking in the software 3D SLICER (Rolfe *et al.* 2021) using the ALPACA extension (Porto *et al.* 2021). ALPACA requires the selection of a 3D reference mesh (source) from which it creates template point clouds through global registration steps (Rusu *et al.* 2009). We chose the 3D reference mesh based on the skull integrity, and its shape being close to the mean skull shape determined by a preliminary analysis. This preliminary analysis consisted of an initial automatic landmarking on all individuals, using a well-preserved skull as reference without consideration of its position in the morphospace. This was followed by a preliminary generalized Procrustes analysis (GPA) and subsequent principal component analysis (PCA) on the landmarked skulls (as described in more detail below), after which we could choose a skull positioned at the centre of the morphospace. For the registration steps, we set the point density at 0.5, which automatically defined 724 single-point pseudo-landmarks distributed over the entire 3D skull meshes (Fig. 3). Then, the software produced a deformable registration step on the source point cloud to match the coordinates of the floating surface to the coordinate of the target surface. This allowed corresponding landmarks between source and target meshes to be transferred to all target specimens.

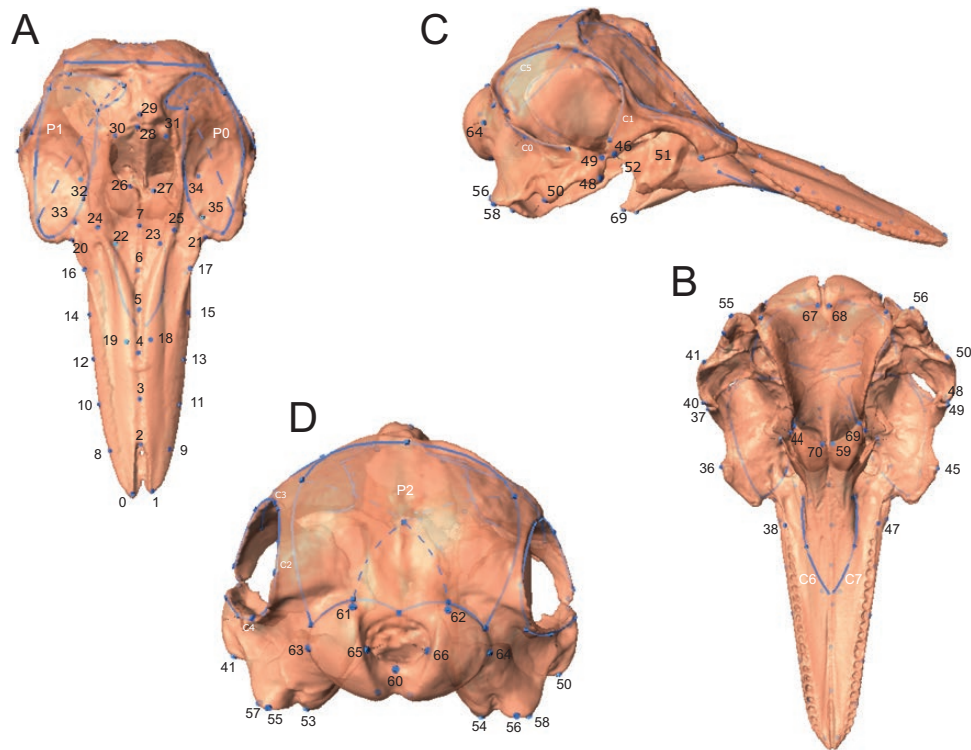


**Figure 2.** Three-dimensional landmarks used in this study, showed in dorsal (A), ventral (B), lateral (C), and occipital (D) aspects of the bottlenose dolphin skull.

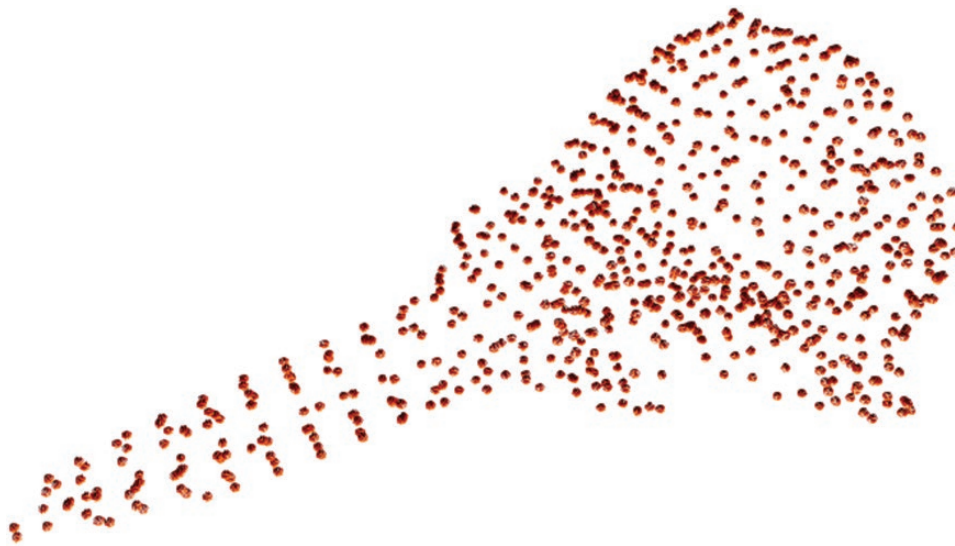


**Figure 3.** 3D LM points generated from the automatic landmarking from the bottlenose dolphin skull reference template.

### Geometric morphometric shape analysis

For both manual and automatic landmark datasets, we performed a GPA. It translated the centroids to a single origin, i.e. centred all shapes, scaled the LMs to the same centroid size, and rotated each shape around the centroid (Rohlf and Slice 1990). This produced a set of aligned Procrustes coordinates for each specimen, on which the effects of size, rotation, and translation were removed. Shape changes between specimens were identified by performing a PCA, which finds the axes of greatest variation in our dataset (principal components—PC),

and groups specimens by similarity across each PC (Rohlf and Marcus 1993; Adams *et al.* 2004). GPA and PCA were performed independently for each of the landmark datasets produced earlier (manual and automatic) using the SLICER extension slicermorph (Rolfe *et al.* 2021). We visualized shape changes associated with PC axes using vector displacement graphs (also known broadly as a lollipop graphs) in slicermorph (Rolfe *et al.* 2021), and coloured each landmark according to their relative rate of change using the software PARAVIEW (Ahrens *et al.* 2005).

To test the differentiation in skull shape, we carried out multiple tests between *a priori* defined groups, which were implemented in the software PAST (Hammer *et al.* 2001). First, we determined five *a priori* groups distinguishing both habitat and geographic origin. The Guayaquil group consisted of specimens determined previously to belong to a resident population of the inner estuary of the Gulf of Guayaquil, based on behavioural, morphological, and genetic criteria (Félix 1997; Bayas-Rea *et al.* 2018; Félix *et al.* 2019). Individuals from Ecuador that were determined as not being part of this resident population were categorized as being offshore specimens from the south-east Pacific (OSEP). Further offshore groups included specimens sampled along the coast of Brazil, known to be taxonomically distinct from the local coastal ecotype (Costa *et al.* 2016; named Offshore South Atlantic—OSA), and specimens from the Atlantic coast of France (named Offshore North Atlantic—ONA). Finally, the Mediterranean group included specimens from the Mediterranean Sea along the Ligurian and Adriatic coasts. Since our tests showed no clear differentiation between the three *a priori* geographically distinct offshore groups (i.e. OSEP, OSA, ONA; see Results for more details, and Supporting Information Fig. S1), they were then clustered into a single *a priori* group consisting of offshore specimens.

All tests were based on the first 55 principal components (PC) scores as they represent approximately 95% of the total variance in our data. First, a non-parametric multivariate analysis of variance test (PERMANOVA) was performed on the PC scores. Additionally, we carried out a linear discriminant analysis (LDA) on the first 55 PC scores. This method carries a pairwise comparison between all defined groups to test how well individual specimens can be classified to their defined group according to their skull shapes. We considered groups to represent different morphotypes when results from the LDA specified that 90% or more of all specimens could be assigned to their respective groups.

We also carried out a hierarchical cluster analysis (HCA), which clusters the skulls based on their shape similarity defined by the first 55 PCs, without consideration of *a priori* groups. Ward's method was used as a clustering procedure.

#### Alveoli count

In addition to the landmarking, we also counted tooth alveoli numbers for both left and right upper tooth rows. When the rostrums were broken or tooth alveoli were undetectable, we did not include the individual in the analysis. Tests for differences in the alveoli counts between the *a priori* groups were carried out in the software PAST (Hammer *et al.* 2001). Normality tests for each *a priori* group were first carried out using the Shapiro–Wilk test, while homogeneity of variances was assessed through a Levene's test. Because data were not normally distributed and had unequal variances, differences in alveoli count were tested using a non-parametric Kruskal–Wallis test, with pairwise differences between groups assessed using the Dunn's post-hoc test.

## RESULTS

The PCA morphospace results for the manual and automatic landmarking approaches are largely consistent in the patterns of shape differentiation between the samples analysed.

However, there are differences in the resulting level of differentiation. Therefore, we present the PCA results from the automatic landmarking in the main text below, showing both results only when the downstream analyses are different. PCA and vector displacement graphs for manual landmarking are shown in the Supporting Information, Figs S2, S4 and S6.

#### Shape variation between locations

The first three principal components together account for 24.9% of the total shape variation (PC1 = 10.6%, PC2 = 8.4%, PC3 = 5.9%) using the automatic landmarking. The PCA morphospace plot reveals that the strongest differentiation is between specimens from the Gulf of Guayaquil and specimens from the Mediterranean (Fig. 4). Both locations also separate well from confirmed offshore individuals, although there is more overlap between the Mediterranean and offshore specimens (Fig. 4). Visual analyses of the plot did not reveal any noticeable separation between offshore specimens from different regions (see Results further down for statistical testing results; Supporting Information, Fig. S1). PCA plot based on manual landmarking shown in Supporting Information, Fig. S2.

In terms of shape change, along PC1, a relative elongation of the rostrum is noticeable, with most changes occurring on the tip of the rostrum and the base of the rostrum, where elongation and narrowing of the palate are noticeable, with an accompanying expansion of the pterygoid bones. There is also a noticeable expansion of the supra-occipital region, causing an apparent contraction of the upper parietal bone. There is also a relative upward shift of the squamosal bone, which collectively would lead to a noticeable change in the shape of the temporal fossae (Fig. 4A; Supporting Information, Fig. S3). Along PC2, there is a noticeable lengthening of the rostrum, with an apparent narrowing and elongation of the upper part of the premaxillae. There is a pronounced contraction upward of the pterygoid bones, and a deepening of the ascending process of the maxilla is also visible (Fig. 4B; Supporting Information, Fig. S3). Along PC3, there is a shortening of the rostrum with an accompanying forward shift in the upper part of the premaxillae near the internal nares. There is also a visible extension backward of the lower edge of the temporal fossae, involving shifts of the frontal, squamosal, and temporal bones, accompanied by a compression of the occipital bone. Overall, specimens with positive PC3 values showed convex curving of the rostral area, with a more prominent rostral bump (Fig. 4C; Supporting Information, Fig. S3). Corresponding shape change plots based on manual landmarking available in Supporting Information, Fig. S4).

Overall, coastal specimens from the Mediterranean show a slender and longer skull, as revealed by the greater interlandmark distances in the rostrum, parietal, and pterygoid areas (Supporting Information, Fig. S5). Individuals from the Gulf of Guayaquil have stouter skulls than the offshore and coastal specimens from the Mediterranean, as revealed by the shortening of the frontal areas and a broadening of the exoccipital region (Fig. 4; Supporting Information, Fig. S5). Corresponding shape change plots based on manual landmarking, available in Supporting Information, Fig. S6.

In our dataset, three skulls showed considerable separation of the maxillary and premaxillary bones along the mid-palate

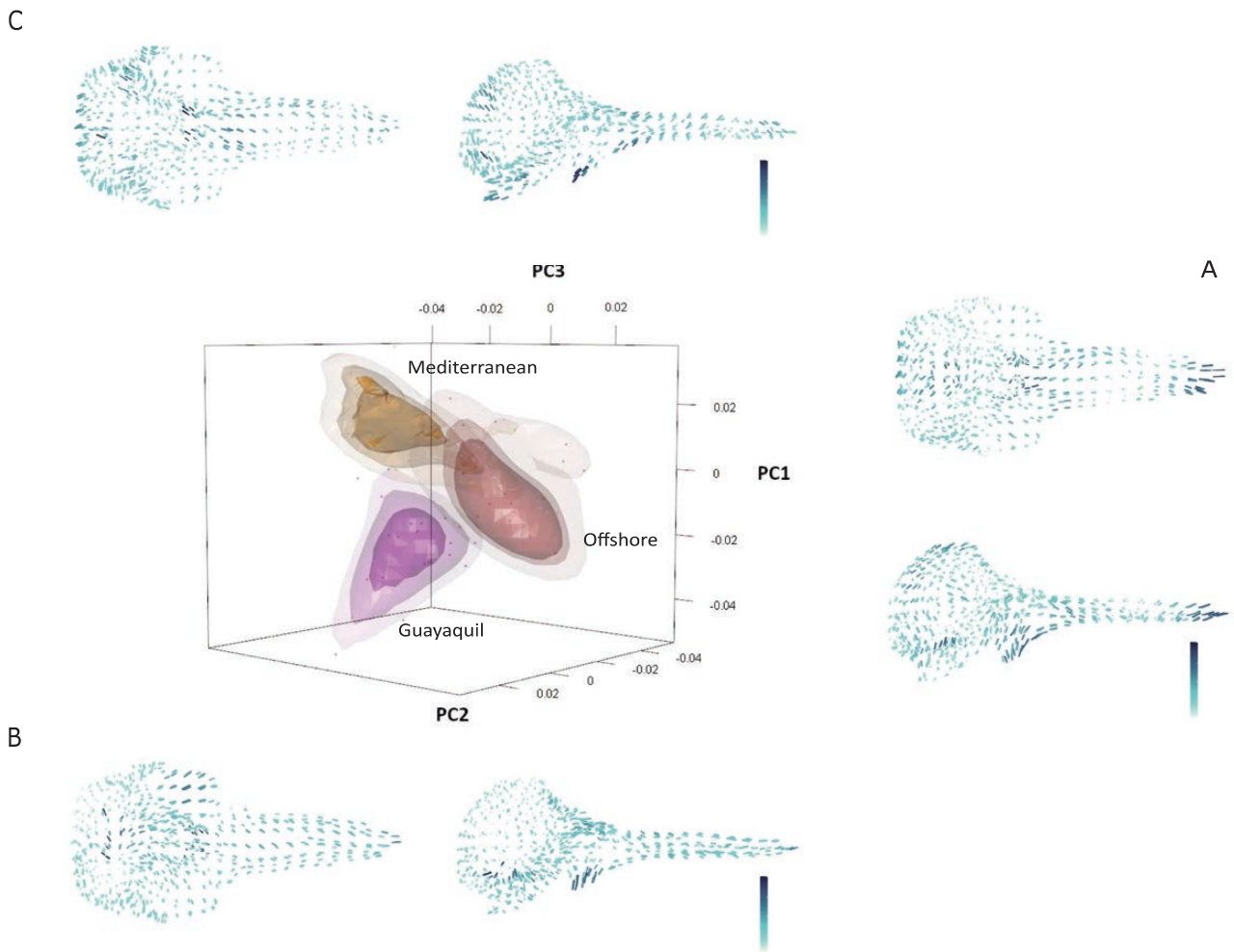


**Figure 4.** 3D PCA morphospace generated from the automatic landmarking procedure, with samples categorized by *a priori* groups. Shaded areas correspond to 90% kernel density clouds for each cluster, as calculated in the R package KS (Duong 2007). Line graphs around the PCA plot represent vector displacement graphs, which represent the difference in landmark position between the mean landmark configuration and specimens grouped along the positive PC1 (A), PC2 (B), and PC3 (C). Darker colour shows a higher rate of shape change for the corresponding landmark.

suture. This is a common modification in delphinid museum specimens resulting from drying of the bones over time, and it was not controlled for in our analyses. However, careful evaluation of the PCA plots revealed that the skulls containing this modification did not cluster together and were not ecotype-specific. This modification was also not shown in the shape deformation grids for the principal components explaining most of the variation. Therefore, although this deformation occurs in our dataset, it is unlikely to influence the conclusions regarding ecotype grouping. However, we cannot exclude other potential biases that might result from this issue in our dataset.

#### Statistical differentiation tests

Pairwise PERMANOVA analysis among the five *a priori* defined geographic groups found no significant differentiation in shape among the three *a priori* offshore groups (OSEP, OSA, ONA), but significant differentiation was observed between Gulf of Guayaquil and Mediterranean Sea with the other groups (Table 1). The significant differentiation between offshore and both Guayaquil and Mediterranean coastal groups was still present when all offshore specimens were pooled into a single

group (Table 2). We should note that there was no difference in the statistical testing between the manual and the automatic landmarking datasets. The linear discriminant function analysis on the first 55 PC scores discriminating offshore ( $N = 18$ ), Gulf of Guayaquil ( $N = 22$ ), and the coastal Mediterranean ( $N = 18$ ) specimens showed that all specimens could be correctly assigned to their respective groups when using both manual and automatic landmarking (Fig. 5).

The HCA shows some differences between the manual and automatic datasets. Both identify three main clusters among all specimens (Table 3), but the relationships estimated between those clusters change slightly (Fig. 6). When using automatic LMs, 77.3% of the Guayaquil specimens (Total  $N = 22$ ) are assigned to cluster 1, whereas 38.9% of offshore specimens (Total  $N = 18$ ) are assigned to cluster 2, and 88.9% of the Mediterranean specimens (Total  $N = 18$ ) are assigned into cluster 3 (Table 3). Although more offshore individuals are assigned to cluster 3 than cluster 2, cluster 2 is still mostly represented by offshore specimens (63.6%) when compared to the other groups. When using manual LMs, 90.9% of the Guayaquil specimens (Total  $N = 22$ ) are again assigned to cluster 1, whereas 77.8% of Mediterranean

specimens (Total  $N = 18$ ) and 61.1% of the offshore specimens (Total  $N = 18$ ) are now assigned to distinct clusters: cluster 2 and cluster 3, respectively (Table 3). Therefore, both datasets show good correspondence between clusters identified and our ecotype assignment, although the automatic landmarking groups more offshore specimens in the same cluster as the Mediterranean specimens. The two datasets also show different relationships in shape similarity between the three clusters. The

automatic landmarking separates the Guayaquil specimens more clearly from both offshore and Mediterranean groups (Fig. 6A). However, the automatic landmarking places the offshore cluster closer to Guayaquil in shape similarity, with the Mediterranean being the most distinct (Fig. 6A). On the contrary, manual landmarking appears to place the Mediterranean cluster closer to the offshore one, but shows less cross-classification between both clusters (Fig. 6B).

**Table 1.** Pairwise PERMANOVA analysis on the first 55 PCs of principal component analysis (PCA) between *a priori* groups separating both habitat and geographical areas. Results are shown for both manual (regular text) and automatic (bold text) landmarks. *F*-values are shown above the empty diagonal cells, while *P*-values are shown below the empty diagonal cells. Significant comparisons are marked by an asterisk (\*). Population abbreviations: OSEP—Offshore Southeast Pacific; ONA—Offshore North Atlantic; OSA—Offshore South Atlantic.

	Mediterranean	Guayaquil	OSEP	OSA	ONA
Mediterranean		9.208*/ <b>4.614*</b>	2.195*/ <b>1.628*</b>	3.277*/ <b>1.968*</b>	2.633*/ <b>1.383</b>
Guayaquil	< 0.001*/< <b>0.001*</b>		4.228*/ <b>2.966*</b>	2.425*/ <b>2.754*</b>	2.914*/ <b>1.849*</b>
OSEP	< 0.001*/ <b>0.010*</b>	< 0.001*/< <b>0.001*</b>		1.406/ <b>1.092</b>	1.329/ <b>1.230</b>
OSA	< 0.001*/ <b>0.002*</b>	< 0.001*/< <b>0.001*</b>	0.061/ <b>0.284</b>		1.155/ <b>1.332</b>
ONA	0.001*/ <b>0.054</b>	< 0.001*/ <b>0.002*</b>	0.080/ <b>0.122</b>	0.252/ <b>0.120</b>	

**Table 2.** Pairwise PERMANOVA analysis on the first 55 PCs of principal component analysis (PCA), between *a priori* groups separating both coastal habitats from the offshore habitat using manual (regular text) and automatic (bold text) landmarks. *F*-values are shown above the empty diagonal cells, while *P*-values are shown below the empty diagonal cells. Significant comparisons are marked by an asterisk (\*).

	Mediterranean	Guayaquil	Offshore
Mediterranean		9.208*/ <b>4.614*</b>	3.676*/ <b>2.168*</b>
Guayaquil	< 0.001*/< <b>0.001*</b>		5.018*/ <b>3.673*</b>
Offshore	< 0.001*/< <b>0.001*</b>	< 0.001*/< <b>0.001*</b>	

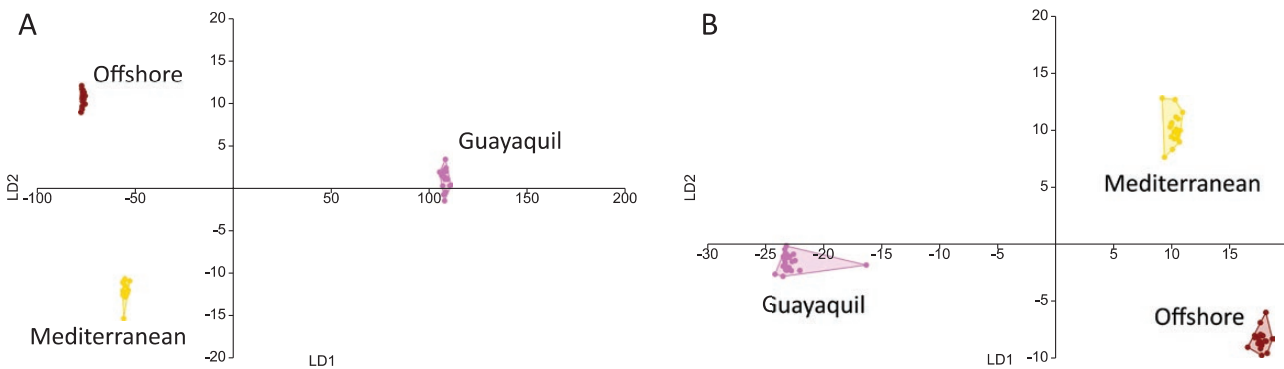


**Figure 5.** Linear discriminant analysis (LDA) on the first 55 PCs of principal component analysis (PCA) of the three *a priori* groups of bottlenose dolphins, generated from: A, manual landmarking; B, automatic landmarking.

**Table 3.** Distribution of bottlenose dolphin skulls over three clusters as inferred by the hierarchical cluster analyses (HCA). Results are shown for both automatic and manual landmarkings.

	Automatic			Manual		
	Cluster 1	Cluster 2	Cluster 3	Cluster 1	Cluster 2	Cluster 3
Offshore	0%	38.9%	61.1%	16.7 %	22.2 %	61.1 %
Mediterranean	0%	11.1 %	88.9%	5.5 %	77.8 %	16.7 %
Guayaquil	77.3%	9.1%	13.6%	90.9 %	0 %	9.1 %

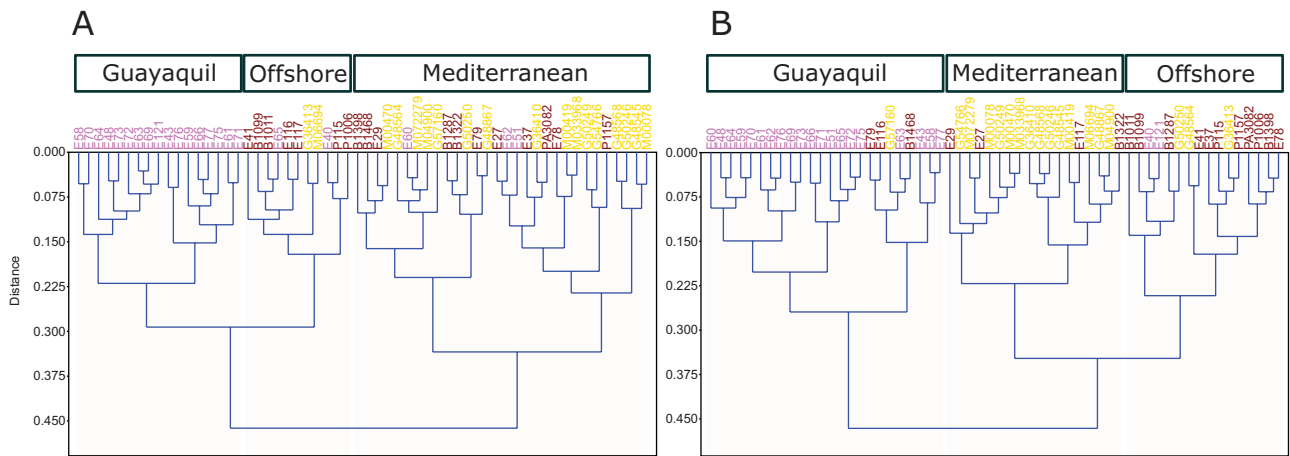


**Figure 6.** Ward's clustering analysis based on the first 55 PCs of principal component analysis (PCA) Euclidean distances: A, automatic landmarking; B, manual landmarking. Location shown indicates the origin of the majority of specimens within each cluster.

### Alveoli counts

The Guayaquil dolphins have fewer alveoli than the Mediterranean and the offshore specimens. Guayaquil have a mean 18.9 alveoli on each tooth row of the maxillae (range 18–22), while the Mediterranean and the offshore specimens have mean 22.7 and 21.8 alveoli, respectively (range 20–25 and 20–23, respectively). Kruskal–Wallis test shows significant differences between the groups ( $H = 29.89$ ;  $P$ -value =  $2.3 \times 10^{-8}$ ). Pairwise Dunn's test shows significant differences between the Guayaquil and the other groups (all  $P$ -values  $< 0.001$ ), but no significant differences between the Mediterranean and the offshore groups ( $P$ -value = 0.82; Table 4). For some individuals, the alveoli of the first teeth at the tip of the rostrum were not visible. However, these were found in all groups equally, and therefore are unlikely to cause any bias.

### DISCUSSION

Our GM study used a transoceanic approach to identify skull shape variations between coastal and offshore populations of bottlenose dolphins. Our results indicate that specimens from both the Gulf of Guayaquil (Ecuador) and the Mediterranean Sea differentiate well from offshore specimens originating from diverse ocean basins. However, the coastal populations from the Gulf of Guayaquil and the Mediterranean Sea are also clearly divergent from each other, meaning that each possess specific cranial morphological characteristics. There was an overlap observed in the morphospace between coastal and offshore specimens in both locations, although the overlap was more noticeable in specimens from the Mediterranean Sea.

Overall, coastal specimens differed from the offshores through the shape and length of their rostrum, the area surrounding the ascending processes of the maxilla, pterygoid bones and occipital regions. Results showed a relative shortening and broadening of Guayaquil dolphins' rostrums, a ventrodorsal contraction of the supraoccipital region, as well as lengthening downward of the pterygoid hamuli. These shape changes made the Guayaquil skulls appear generally stouter when compared to the offshore specimens (all changes refer to shape, as the analyses removed the effect of size). On the

**Table 4.** Pairwise Dunn's test results for comparison between *a priori* groups of teeth alveoli counts.  $P$ -values are shown above the empty diagonal cells, while  $Z$ -statistic is shown below the empty diagonal cells. Significant comparisons are marked by an asterisk (\*).

	Offshore	Mediterranean	Guayaquil
Offshore		0.82	$1.31 \times 10^{-6*}$
Mediterranean	0.23		$2.36 \times 10^{-7*}$
Guayaquil	4.84*	5.17*	

contrary, Mediterranean skulls displayed a slender shape, with a relative lengthening of their rostrums and occipital region relative to offshore specimens. Skull shape changes that appeared similar in both coastal populations relative to offshore include a broadening and lengthening of the upper part of the maxillae and premaxillae sac fossae, a frontward compression of the lower edge of the temporal fossae, a flattening of the lacrimal process (an exoccipital region further oriented toward the inside of the skull), and a lengthening of the posterior edge of the pterygoid hamulus. The pterygoid, though, was more aligned with the rest of the skull in the Mediterranean dolphins, while in Guayaquil individuals there was a more acute angle with the sagittal plane of the skull.

These results are consistent with previous morphometric studies on *Tursiops truncatus*, which found skull morphological differences between coastal and offshore environments around the world (Mead and Potter 1995; Turner and Worthy 2003; Santillán *et al.* 2008; Viaud-Martinez *et al.* 2008; Perrin *et al.* 2011; Costa *et al.* 2016; Hohl *et al.* 2020; Esteves-Ponte *et al.* 2022). Along the US Atlantic coast, coastal specimens could be differentiated from offshore by a combination of skull length and width, as well as width of the internal nares (Mead and Potter 1995), features that also distinguish coastal from offshore specimens in this study. In California, the shape of the temporal fossa was also found to differentiate between coastal and offshore specimens (Perrin *et al.* 2011). In this study, we found changes in several bones surrounding the mandibular joint, as well as changes in the supraoccipital, which would result in changes to the shape of the temporal fossa. In the coast of Brazil, another

feature that separated the coastal from offshore specimens was the shape of the premaxillary sac fossa and the prenasal triangle (Costa *et al.* 2016), which is also a feature identified in this study as being different between coastal and offshore specimens. These morphological traits were also found to separate coastal from offshore specimens in the Black Sea (Viaud-Martinez *et al.* 2008) and the Gulf of California (Esteves-Ponte *et al.* 2022). Previous studies with skulls from the south-east Pacific showed differences between coastal and offshore specimens at the anteorbital process, palatine, pterygoids, and form of occipital condyles (Van Waerebeek *et al.* 1990, 2017). Our study also detected changes in the areas involving the pterygoids, the orbital arches, and the basicranium. There were also changes detected in the palate region, associated with an overall shape change in the rostrum. However, our study showed that the magnitude of change was larger for the pterygoid bones and features associated with the shape of the rostrum.

Although our study identified diagnostic changes along common skull traits between coastal and offshore specimens, it shows that different coastal populations can also differ from each other. While previous studies did not always compare their coastal populations to the same offshore specimens, different relative patterns were sometimes reported. For example, while the coastals from the US Atlantic coast were reportedly smaller with a slender rostrum compared to offshores (Mead and Potter 1995; Costa *et al.* 2022), the California coastals appear overall more robust in their skull shapes (Perrin *et al.* 2011). The coastal specimens from Brazil were larger relative to offshore specimens (Costa *et al.* 2016). Our study compares both putative coastal animals against the same offshore specimens, which includes representatives from the Pacific and Atlantic Oceans, and our inference does also suggest that coastal animals from different locations display distinct skull shapes.

In this context, our use of two distinct landmarking strategies also provides insight regarding which context they might be most useful. While both effectively distinguished the two coastal populations, the automatic landmarking suggests that the Mediterranean differentiation is subtler compared to Guayaquil. This is not only consistent with the results obtained in the PCA morphospace, but also consistent with known ecological differences (as discussed below). Thus, while manual landmarking of known features might be more effective at identifying subtle differences in individual cases where differentiation is known to occur, automatic landmarking could be more suitable for the identification of relative patterns of differentiation in broader comparative studies.

### Ecological data supporting local differentiation

The skull shape differentiation found in this study also matches other lines of evidence from those coastal areas. Previous studies on site fidelity and social behaviour in the Gulf of Guayaquil suggest a strong level of demographic independence between animals found frequently in the inner estuary of the Gulf, as opposed to the ones found outside the Gulf (Félix *et al.* 2019). Studies on mtDNA differentiation also show evidence of genetic differentiation, suggesting reduced gene flow between those two ecotypes (Bayas-Rea *et al.* 2018).

The Ligurian sea, where most of the specimens analysed in this study originated, was also suggested to include a localized social unit that is demographically independent of animals found in Sicily (Gnone *et al.* 2011; Carnabuci *et al.* 2016; Rossi *et al.* 2017; Terranova *et al.* 2021). In the Mediterranean Sea, genetic studies show population structuring from the Black Sea to the Atlantic, with genetic breaks matching environmental barriers (Natoli *et al.* 2005). The occurrence of individuals with a genetic profile typical of Atlantic offshore animals suggests the occurrence of the offshore ecotype within the Mediterranean (Gaspari *et al.* 2015b). Although bottlenose dolphins in the Mediterranean are more frequently sighted in nearshore waters (Bearzi *et al.* 2008; Gnone *et al.* 2011; Marini *et al.* 2015; Karamitros *et al.* 2020; ACCOBAMS 2021), the larger overlap in shape observed between the Mediterranean and offshore specimens suggests the occurrence of offshore animals in the Mediterranean and is consistent with a potential metapopulation dynamic in the region (Nichols *et al.* 2007; Gaspari *et al.* 2015b; Carnabuci *et al.* 2016).

### Functional role of observed morphological changes

Our 3DGM approach allowed us to identify the main areas of skull shape change between these groups, showing that most changes involve rostrum shape, the concavity of the interorbital shield, and the shape of bones surrounding the mandibular joint. Those features naturally suggest roles for differences in feeding and sound production (as the interorbital shield accommodates the melon and associated musculature) (Harper *et al.* 2008).

Similar interpretations have been proposed by earlier studies, with suggestions that differences in prey size might be particularly relevant (McCurry *et al.* 2017a). In animals showing exaggerated extension of the rostrum (such as dolphins), the rostrum and the mandibular joint were shown to be areas of high mechanical strain (McCurry *et al.* 2017c). Longer and more robust rostrums with a higher number of teeth were often associated with dolphins' ability to capture large demersal prey living in coastal environments (Perrin *et al.* 2011; Costa *et al.* 2016). In addition, larger temporal fossae and maxillae in those individuals would permit the attachment of larger temporal muscles, allowing a more potent bite force when depredating larger prey (Perrin *et al.* 2011; Cozzi *et al.* 2016; Galatius *et al.* 2020).

Dolphins from the Gulf of Guayaquil have been reported to prey on demersal fish, such as sciaenids and small pelagic species (Félix 1994), but also a variety of other species including mullets, catfish, snooks, and carangids, as observed during feeding periods (Félix, unpublished data). They also often show strand-feeding behaviour, which is seen relatively rarely in this species (Jiménez and Alava 2015). There is no information on potential prey for offshore bottlenose in Ecuador, but studies elsewhere in the Pacific suggest a preference for small pelagic and mesopelagic fish (Walker *et al.* 1999; Van Waerebeek *et al.* 2017). Stomach content studies show that Mediterranean animals predominantly consume demersal fish, while offshore appear to feed on a mixture of pelagic fish and cephalopods (Martin 1986; Blanco *et al.* 2001; Santos *et al.* 2001; Bearzi *et al.* 2008). Differences in prey size have been suggested to be an important driver of skull shape changes in delphinids more broadly (Perrin *et al.* 2011; McCurry *et al.* 2017b) and, therefore, prey size differences could also be driving the skull shape differences described here.

Another important ecological difference that could be driving these skull differences is the behaviour required to exploit locally abundant prey. In Delphinids, the hamuli are directly involved in sound production (Cozzi *et al.* 2016), and a previous study suggested that thicker and longer hamuli in offshore specimens could facilitate tracking of smaller and more challenging prey via echolocation (Perrin *et al.* 2011). Similarly, modifications of the maxillae were associated with specific sound emission and reception, and some authors have argued that larger premaxillae and interorbital shields (maxillae and lacrimals involved) could act as a reflector in dolphins (Geisler *et al.* 2014). Coastal dolphins in the Gulf of Guayaquil live in an environment with poor visibility due to the sediment charge of rivers, which could demand more frequent use of echolocation compared to other environments with better visibility.

In this study, offshore specimens showed a more prominent rostral bump and more concave premaxillae at the interorbital shield region. This area corresponds to the melon attachment area (Harper *et al.* 2008). Previous studies identified divergences in whistle patterns between populations of bottlenose dolphins living in different Mediterranean basins (La Manna *et al.* 2020). Therefore, the changes in rostral bump found in the offshore specimens relative to those of the Mediterranean could be related to divergent acoustic requirements associated with their differing ecology. The higher concavity of the premaxillae suggests a potentially larger melon, although we lack concrete data to support this. A study comparing external morphology in Brazil concluded that offshore animals had a proportionally shorter rostrum relative to coastal, which translates into a noticeably larger melon, although no direct melon measurements were taken (Simões-Lopes *et al.* 2019).

It is common for the bottlenose dolphin to develop complex behaviours associated with specific foraging techniques. These foraging techniques can be habitat-specific and have, in some cases, been learned socially (Gazda *et al.* 2005; Pennino and Floris 2013; Whitehead and Rendell 2014). Therefore, we hypothesize that distinct environments could require different behavioural strategies for effective survival. The Mediterranean Sea is a large and heterogenous body of water, although it is generally oligotrophic with high oxygen and salt concentrations and low freshwater inputs (Bas 2009; Coll *et al.* 2010). The Ligurian Sea, from where most of the skull specimens used in this study originated from, is a relatively deep basin, with steep, narrow, continental shelf areas in nearby coastlines (Pinardi *et al.* 2006). It is characterized by the convergence of multiple main-water currents, leading to seasonal upwelling (Prieur *et al.* 2020). Conversely, the inner estuary of the Guayaquil Gulf is a small, semi-enclosed body of water, which records high fluctuations in saline composition due to variations in freshwater input yearly (Twilliey *et al.* 2001). There is also a high tidal range (around 3 m) that produces strong currents (up to 100 cm/s). The two coastal environments are, therefore, divergent and may also require specific adaptive behaviours.

## CONCLUSIONS

In this study, we show that 3DGM, using either manual or automatic landmarking, is a useful tool for identifying significant

skull shape differences, not only between dolphins with differing ecologies but also between the coastal specimens of Guayaquil and the Mediterranean. Offshore specimens from different geographical locations showed considerable overlap in skull shape, even between geographically distant areas.

Contrastingly, there was comparatively little overlap between offshore specimens and both coastal populations, although this overlap was noticeably larger in the Mediterranean. Skulls of Guayaquil dolphins looked relatively more robust and had significantly lower tooth count than the offshore and the Mediterranean populations. Contrastingly, the Mediterranean skulls were longer and slenderer compared to others, but did not differentiate in tooth count from offshore specimens. The patterns of shape changes are consistent with previous suggestions that feeding (i.e. prey type and size) and sound production might be ecological drivers. We, therefore, hypothesize that skull differentiation between the two coastal environments may be a response to living in divergent local environments.

Future studies should aim to compare 3D skull shapes between other coastal and offshore ecotypes of bottlenose dolphins. This would improve our understanding of the cranium shape patterns in this clade by analysing the entire 3D surface of each specimen. In addition, more studies are needed on local differences in diets (i.e. stable isotopes or stomach contents), as well as acoustic and genomic composition, providing a deeper insight into the evolutionary ecology of this complex species.

## SUPPLEMENTARY DATA

Supplementary data is available at XXXXXX *Journal* online.

**Table S1.** Accession numbers and details of the specimens used in the analysis.

**Table S2.** The number of individuals per geographical area and habitat type.

**Table S3.** Description of the parameters used for the 3D modelling in MESHROOM.

**Table S4.** Description of the manual LMs used in this study, as shown in Figure 2.

**Figure S1.** 2D PCA morphospace generated from the automatic landmarking procedure, with samples categorized by habitat and geographical area. Specimens from the Gulf of Guayaquil shown in magenta; Offshore from the Southeast Pacific in light blue (OSEP); Offshore from the South Atlantic in dark blue (OSA); Offshore from the North Atlantic in red (ONA); specimens from the Mediterranean Sea in orange.

**Figure S2.** 3D PCA morphospace and kernel density cloud generated from the manual landmarking procedure, with samples categorized by habitat. Offshore populations in red, coastal populations from Guayaquil (Ecuador) in magenta, and from the Mediterranean in orange.

**Figure S3.** Landmark vector displacement plots (Lollipops) between the three ecotypes from the automatic landmarking. Lines represent the difference in landmark position between the mean landmark configuration (black dots) and specimens grouped along the positive PC axis. PC1 is represented in red, PC2 in green and PC3 in blue.

**Figure S4.** Landmark vector displacement plots (Lollipops) between the three ecotypes from the manual landmarking. Lines

represent the difference in landmark position between the mean landmark configuration (black dots) and specimens grouped along the positive PC axis. PC1 is represented in red, PC2 in green and PC3 in blue.

**Figure S5.** 3D PCA morphospace and kernel density cloud generated from the automatic landmarking procedure, comparing Guayaquil vs. offshore specimens only (top), and Mediterranean vs. offshore specimens only (bottom). Landmark vector displacement plots (lollipops) represent the difference in landmark position between the mean landmark configuration and specimens grouped along the positive PC1 (A), PC2 (B), and PC3 (C).

**Figure S6.** Landmark vector displacement plots (lollipops) for manual landmarking between offshore and Guayaquil specimens (left, magenta), and between offshore and Mediterranean (right, orange). Lines represent the difference in landmark position between the mean landmark configuration and specimens grouped along the positive PC axis.

## ACKNOWLEDGEMENTS

This project is funded by the Polish National Science Centre (NCN) Preludium-BIS research grant nr 2019/35/O/NZ8/03900, awarded to AEM, in support of M.D.'s Ph.D. We would also like to thank Dr Kent Mori (National Museum of Nature and Science, Tokyo; The Museum on the Street) for his role in training our research group on the basics of 3D photogrammetry. We also acknowledge the work of all museum staff, who contributed to maintaining the museum collections over the years. A.E.M. was supported by the Polish National Science Centre (Sonata research grant 2018/31/D/NZ8/02835) and the Polish National Agency for Academic Exchange (NAWA Ulam programme PPN/ULM/2019/1/00162).

## FUNDING

This research was funded by the Polish Narodowe Centrum Nauki (NCN), through the Preludium-BIS scholarship number 2019/35/O/NZ8/03900. AEM was further supported by the Narodowe Centrum Nauki (NCN) Sonata programme (nr 2018/31/D/NZ8/02835) and the Narodowa Agencja Wymiany Akademickiej (NAWA) Ulam programme (PPN/ULM/2019/1/00162).

## DATA AVAILABILITY

Landmark data used in this publication are available as a Mendeley dataset, doi: 10.17632/ggkx4jwnmf.1

## CONFLICT OF INTEREST

The authors declare no conflict of interests.

## REFERENCES

- ACCOBAMS. 2021. *Estimates of Abundance and Distribution of Cetaceans, Marine Mega-fauna and Marine Litter in the Mediterranean Sea from 2018–2019 Surveys*. Panigada S, Boisseau O, Canadas A, Lambert C, Laran S, McLanaghan R, Moscrop A (ed.). Monaco: ACCOBAMS Survey Initiative Project, 177.
- Adams DC. Quantitative genetics and evolution of head shape in *Plethodon* salamanders. *Evol Biol* 2011;38:278–86.
- Adams DC, Rohlf FJ, Slice DE. Geometric morphometrics: ten years of progress following the 'revolution'. *Ital J Zool* 2004;71:5–16.
- Ahrens J, Geveci B, Law C. ParaView: an end-user tool for large data visualization. In: Hansen CD, Johnson CR (ed.), *The Visualization Handbook*. Amsterdam: Elsevier, 2005.
- Alcantarilla P, Nuevo J, Bartoli A. Fast explicit diffusion for accelerated features in nonlinear scale spaces. In: Burghardt T, Damen D, Mayol-Cuevas W, Mirmehdi M (ed.), *BMVC 2013—Electronic Proceedings of the British Machine Vision Conference 2013*, 2013.
- Barros NB, Wells RS, Barros NB. Prey and feeding patterns of resident bottlenose dolphins (*Tursiops truncatus*) in Sarasota bay, Florida. *J Mammal* 1998;79:1045–59.
- Bas C. The Mediterranean: a synoptic overview. *Contributions Sci* 2009;5:25–39.
- Bayas-Rea R, Félix F, Montufar R. Genetic divergence and fine scale population structure of the common bottlenose dolphin (*Tursiops truncatus*, Montagu) found in the Gulf of Guayaquil, Ecuador. *PeerJ* 2018;6:e4589.
- Bearzi G, Notarbartolo-Di-Sciara G, Politi E. Social ecology of bottlenose dolphins in the Kvarneric (northern Adriatic Sea). *Mar Mamm Sci* 1997;13:650–68.
- Bearzi G, Politi E, Agazzi S et al. Occurrence and present status of coastal dolphins (*Delphinus delphis* and *Tursiops truncatus*) in the Eastern Ionian Sea. *Aquat Conserv Mar Freshwater Ecosyst* 2005;15:243–57.
- Bearzi G, Fortuna CM, Reeves RR. Ecology and conservation of common bottlenose dolphins *Tursiops truncatus* in the Mediterranean Sea. *Mammal Rev* 2008;39:92–123.
- Blanco C, Salomón O, Raga JA. Diet of the bottlenose dolphin (*Tursiops truncatus*) in the Western Mediterranean Sea. *J Mar Biol Assoc U K* 2001;81:1053–8.
- Borgard HL, Baab K, Pasch B et al. The shape of sound: a geometric morphometrics approach to laryngeal functional morphology. *J Mamm Evol* 2020;27:577–90.
- Borrell A, Vighi M, Genov T et al. Feeding ecology of the highly threatened common bottlenose dolphin of the Gulf of Ambracia, Greece, through stable isotope analysis. *Mar Mamm Sci* 2021;37:98–110.
- Brotos JM, Islas-Villanueva V, Alomar C et al. Genetics and stable isotopes reveal non-obvious population structure of bottlenose dolphins (*Tursiops truncatus*) around the Balearic Islands. *Hydrobiologia* 2019;842:233–47.
- Buser TJ, Sidlauskas BL, Summers AP. 2D or not 2D? Testing the utility of 2D vs. 3D landmark data in geometric morphometrics of the sculpin subfamily Oligocottinae (Pisces; Cottoidea). *Anat Rec* 2018;301:806–18.
- Carnabuci M, Schiavon G, Bellingeri M et al. Connectivity in the network macrostructure of *Tursiops truncatus* in the Pelagos sanctuary (NW Mediterranean Sea): does landscape matter? *Popul Ecol* 2016;58:249–64.
- Christiansen P. Evolution of skull and mandible shape in cats (Carnivora: Felidae). *PLoS One* 2008;3:e2807.
- Coll M, Piroddi C, Steenbeek J et al. The biodiversity of the Mediterranean Sea: estimates, patterns, and threats. *PLoS One* 2010;5:e11842.
- Cooke SB. Paleodiet of extinct platyrrhines with emphasis on the Caribbean forms: three-dimensional geometric morphometrics of mandibular second molars. *Anat Rec* 2011;294:2073–91.
- Cooke SB, Terhune CE. Form, function, and geometric morphometrics. *Anat Rec* 2015;298:5–28.
- Costa A, Rosel P, Daura-Jorge F et al. Offshore and coastal common bottlenose dolphins of the western South Atlantic face-to-face: what the skull and the spine can tell us. *Mar Mamm Sci* 2016;32:1433–57.
- Costa AP, Fruet PF, Secchi ER et al. Ecological divergence and speciation in common bottlenose dolphins in the Western South Atlantic. *J Evol Biol* 2021;34:16–32.
- Costa APB, Mcfee W, Wilcox LA et al. The common bottlenose dolphin (*Tursiops truncatus*) ecotypes of the western North Atlantic revisited: an integrative taxonomic investigation supports the presence of distinct species. *Zool J Linn Soc* 2022;196:1608–36.
- Cozzi B, Huggenberger S, Oelschläger H. Head and senses. In: Cozzi B, Huggenberger S, Oelschläger H (eds), *Anatomy of Dolphins: Insights into Body Structure and Function*. London: Academic Press, 2016, 133–196.

- Díaz-Gamboa RE, Gendron D, Busquets-Vass G. Isotopic niche width differentiation between common bottlenose dolphin ecotypes and sperm whales in the Gulf of California. *Mar Mamm Sci* 2018;**34**:440–57.
- Duong T. Ks: kernel density estimation and kernel discriminant analysis for multivariate data in R. *J Stat Softw* 2007;**21**:1–16.
- Esteves-Ponte MA, Aurióles-Gamboá D, García-Rodríguez FJ. Skull morphometric variability related to offshore and inshore ecotypes of the common bottlenose dolphin (*Tursiops truncatus*) from northwestern Mexico. *Mar Mamm Sci* 2022;**38**:1088–103.
- Fabre AC, Cornette R, Huyghe K *et al.* Linear versus geometric morphometric approaches for the analysis of head shape dimorphism in lizards. *J Morphol* 2014;**275**:1016–26.
- Félix F. Ecology of the coastal bottlenose dolphin *Tursiops truncatus* in the Gulf of Guayaquil, Ecuador. *Investigations on Cetacea* 1994;**25**:235–56.
- Félix F. Organization and social structure of the coastal bottlenose dolphin *Tursiops truncatus* in the Gulf de Guayaquil, Ecuador. *Aquat Mamm* 1997;**23**:1–16.
- Félix F, Burneo S. Imminent risk of extirpation for two bottlenose dolphin communities in the Gulf of Guayaquil, Ecuador. *Front Mar Sci* 2020;**7**:1–17.
- Félix F, Calderón A, Vintimilla M *et al.* Decreasing population trend in coastal bottlenose dolphin (*Tursiops truncatus*) from the Gulf of Guayaquil, Ecuador. *Aquat Conserv Mar Freshwater Ecosyst* 2017;**27**:856–66.
- Félix F, Centeno R, Romero J *et al.* Prevalence of scars of anthropogenic origin in coastal bottlenose dolphin in Ecuador. *J Mar Biol Assoc U K* 2018;**98**:1177–86.
- Félix F, Zavala M, Centeno R *et al.* Spatial distribution, social structure and conservation threats of a small community of bottlenose dolphins, *Tursiops truncatus* (Odontoceti: Delphinidae) in Ecuador. *Revista de Biología Tropical* 2019;**67**:1059–76.
- Fernández R, García-Tiscar S, Santos MB *et al.* Stable isotope analysis in two sympatric populations of bottlenose dolphins *Tursiops truncatus*: evidence of resource partitioning? *Mar Biol* 2011;**158**:1043–55.
- Forcada J, Gazo M, Aguilar A *et al.* Bottlenose dolphin abundance in the NW Mediterranean: addressing heterogeneity in distribution. *Mar Ecol Prog Ser* 2004;**275**:275–87.
- Forrest FL, Plummer TW, Raam RL. Ecomorphological analysis of bovid mandibles from Laetoli Tanzania using 3D geometric morphometrics: implications for hominin paleoenvironmental reconstruction. *J Hum Evol* 2018;**114**:20–34.
- Galatius A, Goodall RNP. Skull shapes of the Lissodelphininae: radiation, adaptation and asymmetry. *J Morphol* 2016;**277**:776–85.
- Galatius A, Berta A, Frandsen MS *et al.* Interspecific variation of ontogeny and skull shape among porpoises (Phocoenidae). *J Morphol* 2011;**272**:136–48.
- Galatius A, Racicot R, McGowen M *et al.* Evolution and diversification of delphinid skull shapes. *iScience* 2020;**23**:101543.
- Gannon DP, Waples DM. Diets of coastal bottlenose dolphins from the U.S. Mid-Atlantic coast differ by habitat. *Mar Mamm Sci* 2004;**20**:527–45.
- Gao T, Kovalsky SZ, Boyer DM *et al.* Gaussian process landmarking for three-dimensional geometric morphometrics. *SIAM J Math Data Sci* 2019;**1**:237–67.
- Gaspari S, Holcer D, Mackelworth P *et al.* Population genetic structure of common bottlenose dolphins (*Tursiops truncatus*) in the Adriatic Sea and contiguous regions: implications for international conservation. *Aquat Conserv Mar Freshwater Ecosyst* 2015a;**25**:212–22.
- Gaspari S, Scheinin A, Holcer D *et al.* Drivers of population structure of the bottlenose dolphin (*Tursiops truncatus*) in the Eastern Mediterranean Sea. *Evol Biol* 2015b;**42**:177–90.
- Gazda SK, Connor RC, Edgar RK *et al.* A division of labour with role specialization in group hunting bottlenose dolphins (*Tursiops truncatus*) off Cedar Key, Florida. *Proc R Soc B: Biol Sci* 2005;**272**:135–40.
- Geisler JH, Colbert MW, Carew JL. A new fossil species supports an early origin for toothed whale echolocation. *Nature* 2014;**508**:383–6.
- Gibbs SE, Harcourt RG, Kemper CM *et al.* Niche differentiation of bottlenose dolphin species in South Australia revealed by stable isotopes and stomach contents. *Wildl Res* 2011;**38**:261–70.
- Giménez J, Marçalo A, Ramírez F *et al.* Diet of bottlenose dolphins (*Tursiops truncatus*) from the Gulf of Cadiz: insights from stomach content and stable isotope analyses. *PLoS One* 2017;**12**:e0184673.
- Gnone G, Bellingeri M, Dhermain F *et al.* Distribution, abundance, and movements of the bottlenose dolphin (*Tursiops truncatus*) in the Pelagos Sanctuary MPA (northwest Mediterranean Sea). *Aquat Conserv Mar Freshwater Ecosyst* 2011;**21**:372–88.
- Gray H, Van Waerebeek K, Owen J *et al.* Evolutionary drivers of morphological differentiation among three bottlenose dolphin lineages, *Tursiops* spp. (Delphinidae), in the Northwest Indian ocean utilizing linear and geometric morphometric techniques. *Biol J Linn Soc* 2022;**135**:610–29.
- Griwodz C, Gasparini S, Calvet L, Gurdjos P, Castan F, Maujean B, Lillo GD, Gasparini S, Calvet L, Gurdjos P, Castan F, Maujean B, Lanthony Y, De Lillo G. AliceVision Meshroom: An open-source 3D reconstruction pipeline. *Proc. 12th ACM Multimed Syst Conf* 2021.
- Hammer O, Harper DAT, Ryan PD. PAST: paleontological statistics software package for education and data analysis. *Palaeontol Electronica* 2001;**4**:1–9.
- Harper CJJ, McLellan WAA, Rommel SAA *et al.* Morphology of the melon and its tendinous connections to the facial muscles in bottlenose dolphins (*Tursiops truncatus*). *J Morphol* 2008;**269**:820–39.
- Hersh SL, Duffield DA. Distinction between northwest Atlantic offshore and coastal bottlenose dolphins based on hemoglobin profile and morphometry. In: Leatherwood S, Reeves RR (eds), *The Bottlenose Dolphin*. Amsterdam: Elsevier, Academic Press, 1990, 129–40.
- Hoelzel AR, Potter CW, Best PB. Genetic differentiation between parapatric nearshore and offshore populations of the bottlenose dolphin. *Proc R Soc Lond Ser B: Biol Sci* 1998;**265**:1177–83.
- Hohl LSL, Sicuro FL, Wickert JC *et al.* Skull morphology of bottlenose dolphins from different ocean populations with emphasis on South America. *J Morphol* 2020;**281**:564–77.
- Jedensjö M, Kemper CM, Krützen M. Cranial morphology and taxonomic resolution of some dolphin taxa (Delphinidae) in Australian waters, with a focus on the genus *Tursiops*. *Mar Mamm Sci* 2017;**33**:187–205.
- Jedensjö M, Kemper CM, Milella M *et al.* Taxonomy and distribution of bottlenose dolphins (genus *Tursiops*) in Australian waters: an osteological clarification. *Can J Zool* 2020;**98**:461–79.
- Jiménez PJ, Alava JJ. Strand-feeding by coastal bottlenose dolphins (*Tursiops truncatus*) in the Gulf of Guayaquil, Ecuador. *Latin Am J Aquat Mamm* 2015;**10**:33–7.
- Karamitros G, Gkafas GA, Giantsis IA *et al.* Model-based distribution and abundance of three delphinidae in the Mediterranean. *Animals* 2020;**10**:260.
- Kenney RD. 1990. Bottlenose dolphins off the Northeastern United States. In: Leatherwood S, Reeves RR (eds), *The Bottlenose Dolphin*. Amsterdam: Elsevier, Academic Press, 369–86.
- LaManna G, Rako-Gospic N, Sarà G *et al.* Whistle variation in Mediterranean common bottlenose dolphin: the role of geographical, anthropogenic, social, and behavioral factors. *Ecol Evol* 2020;**10**:1971–87.
- Lawing AM, Polly PD. Geometric morphometrics: recent applications to the study of evolution and development. *J Zool* 2010;**280**:1–7.
- Loy A, Tamburelli A, Carlini R *et al.* Craniometric variation of some Mediterranean and Atlantic populations of *Stenella coeruleoalba* (Mammalia, Delphinidae): a three-dimensional geometric morphometric analysis. *Mar Mamm Sci* 2011;**27**:E65–78.
- Machado FA. Selection and constraints in the ecomorphological adaptive evolution of the skull of living canidae (Carnivora, mammalia). *Am Nat* 2020;**196**:197–215.
- Marini C, Fossa F, Paoli C *et al.* Predicting bottlenose dolphin distribution along Liguria coast (northwestern Mediterranean Sea) through different modeling techniques and indirect predictors. *J Environ Manage* 2015;**150**:9–20.
- Martin AR. Feeding association between dolphins and shearwaters around the Azores Islands. *Can J Zool* 1986;**64**:1372–4.

- McCabe EJB, Gannon DP, Barros NB *et al.* Prey selection by resident common bottlenose dolphins (*Tursiops truncatus*) in Sarasota Bay, Florida. *Mar Biol* 2010;**157**:931–42.
- McCurry MR, Evans AR, Fitzgerald EMGG *et al.* The remarkable convergence of skull shape in crocodylians and toothed whales. *Proc R Soc B: Biol Sci* 2017a;**284**:20162348.
- McCurry MR, Fitzgerald EMG, Evans AR *et al.* Skull shape reflects prey size niche in toothed whales. *Biol J Linn Soc* 2017b;**121**:936–46.
- McCurry MR, Walmsley CW, Fitzgerald EMG *et al.* The biomechanical consequences of longirostry in crocodylians and odontocetes. *J Biomech* 2017c;**56**:61–70.
- Mead J, Potter C. Recognizing two populations of the bottlenose dolphin (*Tursiops truncatus*) of the Atlantic coast of North America—morphologic and ecologic considerations. *IBI Rep* 1995;**5**:31–44.
- Mitteroecker P, Gunz P. Advances in geometric morphometrics. *Evol Biol* 2009;**36**:235–47.
- Moura AE, Shreves K, Pilot M *et al.* Phylogenomics of the genus *Tursiops* and closely related Delphininae reveals extensive reticulation among lineages and provides inference about eco-evolutionary drivers. *Mol Phylogenet Evol* 2020;**146**:106756.
- Natoli A, Peddemors VM, Rus Hoelzel A. Population structure and speciation in the genus *Tursiops* based on microsatellite and mitochondrial DNA analyses. *J Evol Biol* 2004;**17**:363–75.
- Natoli A, Birkun A, Aguilar A *et al.* Habitat structure and the dispersal of male and female bottlenose dolphins (*Tursiops truncatus*). *Proc R Soc B: Biol Sci* 2005;**272**:1217–26.
- Ngqulana SG, Pistorius P, Galatius A *et al.* Variation in cranial morphology of bottlenose dolphins (genus *Tursiops*) off South Africa. *Mar Mamm Sci* 2019a;**35**:617–36.
- Ngqulana SG, Plön S, Galatius A *et al.* Cranial variation in common dolphins *Delphinus* spp. off South Africa, with the inclusion of information from the holotype of *Delphinus capensis*. *Afr J Mar Sci* 2019b;**41**:247–60.
- Nichols C, Herman J, Gaggiotti OE *et al.* Genetic isolation of a now extinct population of bottlenose dolphins (*Tursiops truncatus*). *Proc R Soc B: Biol Sci* 2007;**274**:1611–6.
- Nicolosi P, Loy A. Geometric morphometric methods as complementary tools to investigate variability in common dolphins (*Delphinus* sp.) using museum specimens. *Aquat Conserv Mar Freshwater Ecosyst* 2019;**31**:22–35.
- Otero IR, Delbracio M. Anatomy of the SIFT method, image processing. *Image Process Line* 2014;**4**:370–96.
- Parsons KM, Durban JW, Claridge DE *et al.* Population genetic structure of coastal bottlenose dolphins (*Tursiops truncatus*) in the northern Bahamas. *Mar Mamm Sci* 2006;**22**:276–98.
- Pennino MG, Floris A. Assessing foraging tradition in wild bottlenose dolphins (*Tursiops truncatus*). *Aquat Mamm* 2013;**39**:282–9.
- Pereira LB, Botta S, Teixeira CR *et al.* Feeding ecology of two subspecies of bottlenose dolphin: a tooth tale. *Aquat Ecol* 2020;**54**:941–55.
- Perrin WF, Heyning JE. Rostral fusion as a criterion of cranial maturity in the common dolphin, *Delphinus delphis*. *Mar Mamm Sci* 1993;**9**:195–7.
- Perrin WF, Thieleking JL, Walker WA *et al.* Common bottlenose dolphins (*Tursiops truncatus*) in California waters: cranial differentiation of coastal and offshore ecotypes. *Mar Mamm Sci* 2011;**27**:769–92.
- Pinardi N, Arneri E, Crise A *et al.* The physical, sedimentary and ecological structure and variability of shelf areas in the Mediterranean sea. In: Robinson AR, Brink KH (eds), *The Sea: Ideas and Observations on Progress in the Study of the Seas*. Volume 14: Interdisciplinary Regional Studies and Syntheses. Cambridge, MA: Harvard University Press, 2006, 1243–330.
- Porto A, Rolfe S, Maga AM. ALPACA: a fast and accurate computer vision approach for automated landmarking of three-dimensional biological structures. *Methods Ecol Evol* 2021;**12**:2129–44.
- Prieur L, D'Ortenzio F, Taillander V *et al.* Physical oceanography of the Ligurian Sea. In: Migon C, Nival P, Sciandra A (eds), *The Mediterranean Sea in the Era of Global Change 1: 30 Years of Multidisciplinary Study of the Ligurian Sea*. London: Wiley-ISTE, 2020, 49–78.
- Quérroul S, Silva MA, Freitas L *et al.* High gene flow in oceanic bottlenose dolphins (*Tursiops truncatus*) of the North Atlantic. *Conserv Genet* 2007;**8**:1405–19.
- Richtsmeier JT, DeLeon VB, Lele SR. The promise of geometric morphometrics. *Am J Biol Anthropol* 2002;**119**:63–91.
- Rohlf JF, Marcus LF. A revolution morphometrics. *Trends Ecol Evol* 1993;**8**:129–32.
- Rohlf JF, Slice D. Extensions of the procrustes method for the optimal superimposition of landmarks. *Syst Zool* 1990;**39**:40–59.
- Rolfe S, Pieper S, Porto A *et al.* SlicerMorph: an open and extensible platform to retrieve, visualize and analyse 3D morphology. *Methods Ecol Evol* 2021;**12**:1816–25.
- Rossi A, Scordamaglia E, Bellingeri M *et al.* Demography of the bottlenose dolphin *Tursiops truncatus* (Mammalia: Delphinidae) in the eastern Ligurian Sea (NW Mediterranean): quantification of female reproductive parameters. *Eur Zool J* 2017;**84**:294–302.
- Rusu RB, Blodow N, Beetz M. Fast point feature histograms (FPFH) for 3D registration. *Proc IEEE Int Conf Robot Autom* 2009:3212–7.
- Santillán L, Félix F, Haase B. A preliminary morphological comparison of skulls of common bottlenose dolphins *Tursiops truncatus* from Peru and Ecuador. In: Document SC/60/SH10 presented to the Scientific Committee of the International Whaling Commission, Santiago, Chile, 2008.
- Santos MB, Pierce GJ, Reid RJ *et al.* Stomach contents of bottlenose dolphins (*Tursiops truncatus*) in Scottish waters. *J Mar Biol Assoc U K* 2001;**81**:873–8.
- Sellas AB, Wells RS, Rosel PE. Mitochondrial and nuclear DNA analyses reveal fine scale geographic structure in bottlenose dolphins (*Tursiops truncatus*) in the Gulf of Mexico. *Conserv Genet* 2005;**6**:715–28.
- Simões-Lopes PC, Daura-Jorge FG, Lodi L *et al.* Bottlenose dolphin ecotypes of the western South Atlantic: the puzzle of dorsal fin shapes, colors and habitats. *Aquat Biol* 2019;**28**:101–11.
- Smith KK. Craniofacial development in marsupial mammals: developmental origins of evolutionary change. *Dev Dyn* 2006;**235**:1181–93.
- Terranova F, Gnone G, Friard O *et al.* Signature whistles of the demographic unit of bottlenose dolphins (*Tursiops truncatus*) inhabiting the Eastern Ligurian Sea: characterisation and comparison with the literature. *Eur Zool J* 2021;**88**:771–81.
- Tezanos-Pinto G, Baker CS, Russell K *et al.* A worldwide perspective on the population structure and genetic diversity of bottlenose dolphins (*Tursiops truncatus*) in New Zealand. *J Hered* 2009;**100**:11–24.
- Turner JP, Worthy GAJ. Skull morphometry of bottlenose dolphins (*Tursiops truncatus*) from the Gulf of Mexico. *J Mammal* 2003;**84**:665–72.
- Twilley RR, Cárdenas W, Rivera-Monroy VH *et al.* The gulf of Guayaquil and the Guayas river estuary, Ecuador. In: Seeliger U, Kjerfve B (eds), *Coastal marine ecosystems of Latin America*. Berlin: Springer Science, 2001, 245–63.
- Van Waerebeek K, Reyes JC, Read AJ *et al.* Preliminary observations of bottlenose dolphins from the Pacific coast of South America. Pages 143–154. In: Leatherwood S, Reeves RR (eds), *The Bottlenose Dolphin*. San Diego: Academic Press, 1990, 653.
- Van Waerebeek K, Reyes JC, Sanino GP *et al.* Common bottlenose dolphins *Tursiops truncatus* of Pacific South America, a synoptic review of population identification data. In: IWC Scientific Committee Meeting, Bled, Slovenia, 2017.
- Viaud-Martinez KA, Brownell RL, Komnenou A *et al.* Genetic isolation and morphological divergence of Black Sea bottlenose dolphins. *Biol Conserv* 2008;**141**:1600–11.
- Walker JL, Potter CW, Macko SA. The diets of modern and historic bottlenose dolphin populations reflected through stable isotopes. *Mar Mamm Sci* 1999;**15**:335–50.
- Whitehead H, Rendell L. *The Cultural Lives of Whales and Dolphins*. Chicago: University of Chicago Press, 2014.
- Wiley DF. *Landmark Editor 3.0*. IDAV. Davis: University of California, 2005.